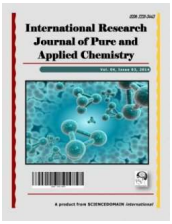

International Research Journal of Pure & Applied Chemistry
14(1): 1-10, 2017; Article no.IRJPAC.32694
ISSN: 2231-3443, NLM ID: 101647669

SCIENCEDOMAIN *international*
www.sciencedomain.org

A Theoretical Study of the Relationships between Electronic Structure and Inhibitory Effects of Caffeine Derivatives on Neoplastic Transformation

Gaston Assongba Kpotin[1*], Gauthier Kankinou[1], Urbain A. Kuevi[1], Juan S. Gómez-Jeria[2] and Jean-Baptiste Mensah[1]

[1]Laboratory of Theoretical Chemistry and Molecular Spectroscopy (LACTHESMO), Faculty of Sciences and Technologies, University of Abomey-Calavi, 01BP1326 Cotonou, Benin.
[2]Quantum Pharmacology Unit, Department of Chemistry, Faculty of Sciences, University of Chile, Las Palmeras 3425, Santiago 7800003, Chile.

Authors' contributions

This work was carried out in collaboration between five authors. Author GAK performed the analysis and wrote the first draft. Author GK performed one part of calculation. Author UAK helped to found the different orbital type. Author JSGJ performed one part of calculation and managed the analysis. Author JBM gave some advices. All authors read and approved the final manuscript.

Article Information

DOI: 10.9734/IRJPAC/2017/32694
Editor(s):
(1) Bengi Uslu, Department Analytical Chemistry, Ankara University, Ankara-Turkey.
Reviewers:
(1) Nagendra Singh, Gautam Buddha University, India.
(2) Gyula Oros, Budapest, Hungary.
(3) Birsa Mihail Lucian, Alexandru Ioan Cuza University of Iasi, Romania.
Complete Peer review History: http://www.sciencedomain.org/review-history/18682

Original Research Article

Received 10th March 2017
Accepted 31st March 2017
Published 18th April 2017

ABSTRACT

A DFT study of the relationships between electronic structure and inhibitory effects of caffeine derivatives on neoplastic transformation was carried out. We obtain one statistically significant equation ($R=0.97$, $R^2= 0.94$, adjusted $R^2= 0.92$, $F(7,34) =71.40$ ($p<0.00001$), $SD=0.14$), relating the variation of the biological activity with the variation of the values of a definite set of local atomic reactivity indices. Based on the analysis of the results, a partial pharmacophore was built that can be employed as a tool for the development of more active molecules. Calculations have been performed by DFT/B3LYP method in the 6-31G orbital basis set.

**Corresponding author: E-mail: gaston.kpotin@fast.uac.bj;*

Keywords: Caffeine; anticancer; QSAR; pharmacophore; DFT; electronic structure.

1. INTRODUCTION

Cancer is a generic term for a large group of diseases that can affect any part of the body. Other terms used are malignant tumors and neoplasms. One defining feature of cancer is the rapid creation of abnormal cells that grow beyond their usual boundaries, and which can then invade adjoining parts of the body and spread to other organs, the latter process is referred to as metastasizing. Metastases are a major cause of death from cancer [1]. There was a worldwide increase of 14 million new cases of different types of cancer in 2012 [1]. The increasing magnitude of the cancer problem is partly the consequence of the population growth and ageing. Such demographic transitions mean that by 2030, well over 20 million new cancer cases will be diagnosed every year [2]. Some studies are directed to found compounds with anticancer activity [3-10]. Previous studies revealed that caffeine inhibits the development of tumors induced by various carcinogens in numerous organs including skin [11], lung [12], breast [13], liver [14] and glioma [15].

Rogozin et al. [16] investigated the potential chemopreventive activities of 50 different 1,3,7-trialkylxanthines which resemble caffeine in their structures but differ in the length of the alkyl side chains. They reported that the number of carbon in two alkyl chain seems to be important for the antitumor-promoting activity.

We present in this paper the results of a QSAR study of caffeine derivatives with inhibition activity on neoplastic transformation. This study was performed with the aim of providing more information about the atomic sites which can be modified to obtain more active molecules.

2. METHODS, MODELS AND CALCULATIONS

2.1 The Method

The methodology employed here to find relationships between electronic structure and inhibition constants has been discussed in several papers [17-24]. The results presented here were obtained from what was a routinary procedure. For this reason, we built a universal model for the paper's structure. This model contains standard phrases for the presentation of the methods, calculations and results because they do not need to be rewritten repeatedly [17-24]. The application of this method has given remarkable results for a great diversity of drug-receptor systems (see [25-39] and references therein).

2.2 Selection of Molecules and Biological Activities

Molecules were selected from a set reported in Ref. [16]. Their general formula and biological activity are displayed, respectively, in Fig. 1 and Table 1. The experimental data employed are inhibitory activities of caffeine on neoplastic transformation, expressed as ICT50. The effect of xantines on EGF- or TPA-induced cell transformations was investigated using JB6 P+ cells. Cells (8103) were exposed to EGF or TPA, with or without xantines (0.005-3 mM), in 1 ml of 0.33% basal medium Eagle agar containing 10% FBS and overlaid with 3.5 ml of 0.5%. The effect of the compounds on transformation of JB6 P+ cells is expressed as a percent inhibition of cell transformation compared with EGF- or TPA-stimulated cells as a positive control [16].

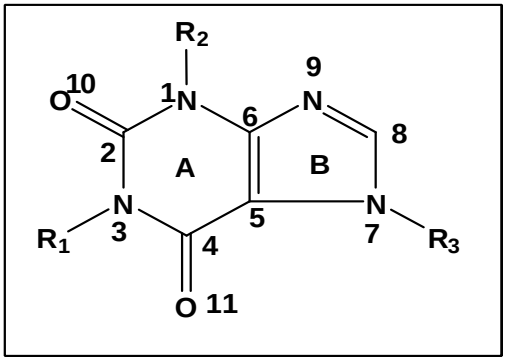

Fig. 1. Structure of caffeine

2.3 Calculations

The electronic structure of all molecules was calculated within the Density Functional Theory (DFT) at the B3LYP/6-31 g level with full geometry optimization. The Gaussian set of programs was used [40]. We used D-Cent-QSAR software [41,42] for the calculation of the numerical values of the local atomic reactivity indices from the Gaussian results. Statistica software [43] was employed for Linear Multiple Regression Analysis (LMRA). All the calculation process is explained in several papers (see ref [25-39]).

Table 1. Selected molecules and their inhibitory activity on neoplastic transformation

N°	R_1	R_2	R_3	log(ICT50)	N°	R_1	R_2	R_3	log(ICT50)
1	Me	Me	Me	2.68	26	n-Pent	n-Bu	H	1.48
2	Me	H	H	2.72	27	H	n-Hex	H	1.70
3	H	H	Me	3.07	28	Me	n-Hex	H	1.30
4	Me	Me	H	2.88	29	n-Hex	Et	H	1.70
5	Me	H	Me	3.10	30	Et	n-Hex	H	1.00
6	Et	H	H	2.69	31	n-Hex	n-Pr	Me	1.48
7	H	Et	H	2.71	32	n-Hex	n-Bu	H	1.48
8	H	n-Pr	Et	2.20	33	H	H	H	2.65
9	Et	n-Pr	H	2.58	34	H	Me	H	2.67
10	Me	n-Pr	Et	2.40	35	H	Me	Me	2.67
11	Et	n-Pr	Me	2.48	36	Et	Me	H	2.38
12	n-Pr	n-Pr	H	2.11	37	Et	Et	H	2.58
13	Me	n-Pr	n-Pr	2.48	38	n-Pr	H	H	2.63
14	n-Bu	H	H	2.83	39	H	n-Pr	H	2.57
15	n-Bu	Me	H	2.48	40	n-Pr	Me	H	2.67
16	Me	n-Bu	H	2.26	41	Me	n-Pr	Me	2.30
17	n-Bu	Et	H	1.70	42	H	n-Pr	Me	2.75
18	Et	n-Bu	H	1.70	43	H	n-Pr	n-Pr	2.52
19	n-Pr	n-Bu	H	2.08	44	H	n-Bu	H	2.46
20	n-Bu	n-Pr	Me	1.70	45	n-Pent	H	H	2.75
21	Me	n-Pr	n-Bu	2.11	46	n-Hex	H	H	2.59
22	n-Bu	n-Bu	H	2.18	47	n-Pr	Et	H	2.08
23	n-Pent	Et	H	1.70	48	n-Pr	n-Pr	Me	2.51
24	Et	n-Pent	H	2.18	49	n-Pent	Me	H	2.00
25	n-Pent	n-Pr	Me	1.60	50	n-Hex	Me	H	2.56

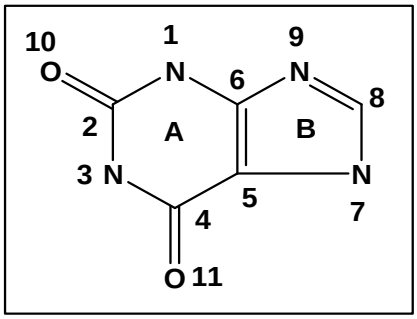

Fig. 2. Common skeleton of caffeine derivatives

We employed the common skeleton hypothesis that holds that there is a certain collection of atoms, common to all molecules analyzed, that accounts for nearly all the biological activity. The action of the substituents consists in modifying the electronic structure of the common skeleton and influencing the right alignment of the drug throughout the orientational parameters. It was conjectured that diverse parts or this common skeleton accounts for almost all the interactions leading to the expression of a given biological activity. The common skeleton for caffeine derivatives is shown in Fig. 2.

3. RESULTS AND DISCUSSION

The best equation obtained was:

$$\log(ICT_{50}) = -12.38 + 20.3F_{10}(LUMO)^{*} - 0.0006\varphi_{R2} + 6.79Q_{4}^{\max} - 0.0003\varphi_{R1} + 50.58F_{5}(LUMO+2)^{*} - 0.97F_{8}(HOMO-2)^{*} - 3.67F_{2}(LUMO+1)^{*} \quad (1)$$

with n=42, R=0.97, R2=0.94, adj-R2=0.92, F(7,34)=71.40 (p<0.00000) and SD=0.14. No outliers were detected and no residuals fell outside the ±2σ limits. Here, $F_{10}(LUMO)^{*}$ is the electron population (Fukui index) of lowest vacant MO localized on atom 10, φ_{R2} is the orientational parameter of the R2 substituent, $Q_4^{\max}$ is the maximum amount of electronic charge that atom 4, φ_{R1} is the orientational parameter of the R1 substituent, $F_5(LUMO+2)^{*}$ is the electron population (Fukui index) of third lowest vacant MO localized on atom 5, $F_8(HOMO-2)^{*}$ is the electron population (Fukui index) of third highest occupied MO localized on atom 8 and $F_2(LUMO+1)^{*}$ is the electron population (Fukui index) of second lowest vacant MO localized on atom 2.

Table 2 shows the beta coefficients and the t-test results for the significance of coefficients of equation 2. Concerning independent variables, Table 3 shows that the highest internal correlation is $r^2(F_{10}(LUMO)^*, Q_4^{max})$=0.27. Fig. 3 displays the plot of observed values vs. calculated values of log(ICT50). The associated statistical parameters of Eq. 1 shows that this equation is statistically significant and explaining about 92% of the variation of the biological activity.

The associated statistical parameters of Eq.1 indicate that this equation is statistically significant and that the variation of the numerical values of a group of seven local atomic reactivity indices of atoms of the common skeleton explains about 92% of the variation of log(ICT50). Fig. 3, spanning about

Table 2. Beta coefficients and t-test for significance of coefficients in equation 1

Variable	Beta coefficients	t(34)	p-Value
$F_{10}(LUMO)^*$	0.27	-5.56	0.000003
φ_{R2}	-0.58	4.12	0.000232
Q_4^{max}	0.18	-11.02	0.000000
φ_{R1}	-0.36	3.19	0.003051
$F_5(LUMO+2)^*$	0.26	-5.91	0.000001
$F_8(HOMO-2)^*$	-0.21	4.81	0.000030
$F_2(LUMO+1)^*$	-0.15	-3.70	0.000761

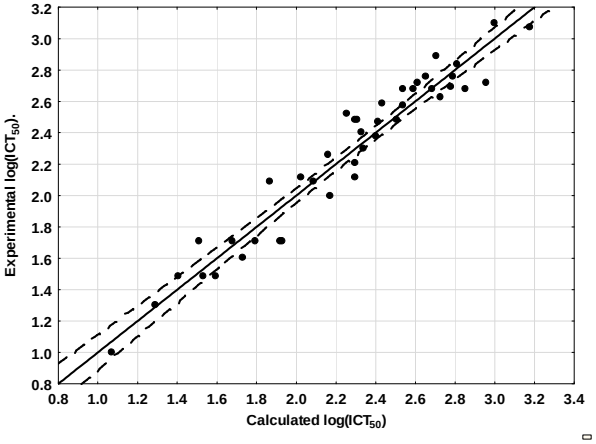

Fig. 3. Plot of predicted vs. observed log(ICT50) values

Table 3. Squared correlation coefficients for the variable appearing in equation 2

	$F_{10}(LUMO)^*$	φ_{R2}	Q_4^{max}	φ_{R1}	$F_5(LUMO+2)^*$	$F_8(HOMO-2)^*$
φ_{R2}	0.10	1.00				
Q_4^{max}	0.27	0.04	1.00			
φ_{R1}	0.21	0.02	0.14	1.00		
$F_5(LUMO+2)^*$	0.00	0.01	0.06	0.02	1.00	
$F_8(HOMO-2)^*$	0.12	0.22	0.01	0.03	0.06	1.00
$F_2(LUMO+1)^*$	0.11	0.10	0.02	0.02	0.10	0.11

2.6 orders of magnitude, shows that there is a good correlation of observed versus calculated values and that almost all points are inside the 95% confidence interval. A significant point to stress is the following. When a local atomic reactivity index of an inner occupied MO (i.e., HOMO-1 and/or HOMO-2) or of a higher vacant MO (LUMO+1 and/or LUMO+2) appears in any equation, this means that the remaining of the upper occupied MOs (for example, if HOMO-2 appears, upper means HOMO-1 and HOMO) or the remaining of the empty MOs (for example, if LUMO+1 appears, lower means the LUMO) contribute to the interaction. Their absence in the equation only means that the variation of their numerical values does not account for the variation of the numerical value of the biological property.

3.1 Local Molecular Orbitals

Table 4 shows the local MO structure of atoms with reactivity indices appearing in Eq. 1 (see Fig. 2). Nomenclature: Molecule (HOMO) / (HOMO-2)* (HOMO-1)* (HOMO)* - (LUMO)* (LUMO+1)* (LUMO+2)*.

Table 4. Local molecular orbitals of atoms 2, 5, 8 and 10

Molecule	Atom 2 (C)	Atom 5 (C)	Atom 8 (C)	Atom 10 (O)
1 (51)	47π50π51π- 53π56π57σ	48π50π51π- 52π53π54π	47σ48π51π- 52π54π55π	49π50π51π- 53π59π68π
2 (43)	38σ40π42π- 45π48π49σ	40π42π43π- 44π45π46π	39π40σ43π- 44π46π47π	41π42π43π- 45π50π54π
3 (43)	38π40π42π- 45π47π51σ	41π42π43π- 44π45π46π	40σ41π43π- 44π46π48π	41π42π43π- 45π49π52π
4 (47)	44π46π47π- 49π52σ53σ	44π46π47π- 48π49π50π	42π43π47π- 48π50π51π	45π46π47π- 49π54π60π
5 (47)	42π43π46π- 49π51σ53σ	44π46π47π- 48π49π50π	43σ44π47π- 48π50π52π	45π46π47π- 49π55π61π
6 (47)	41π44π46σ- 49π52σ53σ	44π46π47π- 48π49π50π	43π44σ47π- 48π50π51π	45π46π47π- 49π55π61π
7 (47)	44π46σ47π- 49π52π53σ	44π46π47π- 48π49π50π	43π44σ47π- 48π49π50π	45π46π47π- 49π55π61π
8 (55)	53π54π55π- 57π59π60σ	53π54π55π- 56π57π58π	52π53π55π- 56π58π60π	53π54π55π- 57π64π71π
9 (59)	56π58π59π- 61π64σ65σ	56π58π59π- 60π61π62π	55π56π59π- 60π62π63π	57π58π59π- 61π67π80π
10 (63)	59π62π63π- 65π68π69σ	60π62π63π- 64π65π66π	60π61π63π- 64π66π67π	61π62π63π- 65π71π84π
11 (63)	60π62π63π- 65π67σ69σ	60π62π63π- 64π65π66π	60π61π63π- 64π66π67σ	61π62π63π- 65π72π87π
12 (63)	60π62π63π- 65π68σ70σ	60π62π63π- 64π65π66π	59π60σ63π- 64π66π67π	61π62π63π- 65π78π86π
13 (67)	63π66π67π- 69π72π73σ	64π66π67π- 68π69π70π	64π65π67π- 68π70π71π	65π66π67π- 69π75π91π
14 (55)	47π52π54π- 57π60π61σ	52π54π55π- 56π57π58π	50σ51π55π- 56π58π59π	53π54π55π- 57π63π69π
15 (59)	56π58π59π- 61π64σ65σ	56π58π59π- 60π61π62π	54σ55π59π- 60π62π63π	57π58π59π- 61π68π77π
16 (59)	56π58π59π- 61π64σ65σ	56π58π59π- 60π61π62π	55π56σ59π- 60π62π63σ	57π58π59π- 61π68π81π
17 (63)	60π62π63π- 65π68π69σ	60π62π63π- 64π65π66π	59π60π63π- 64π66π67π	61π62π63π- 65π72π81π
18 (63)	60π62π63π- 65π68σ69σ	60π62π63π- 64π65π66π	59π60σ63π- 64π66π67π	61π62π63π- 65π72π86π
19 (67)	64π66π67π- 69π72σ74σ	64π66π67π- 68π69π70π	63π64σ67π- 68π70π71π	65π66π67π- 69π77π85π
20 (71)	68π70π71π- 73π75σ78σ	68π70π71π- 72π73π74π	67π68π71π- 72π74π76π	69π70π71π- 73π81π89π
21 (71)	67π70π71π- 73π76σ78σ	68π70π71π- 72π73π74π	68π69π71π- 72π74π75π	69π70π71π- 73π80π100π
22 (71)	68π70π71π- 73π76σ78σ	68π70π71π- 72π73π74π	67π68π71π- 72π74π75π	69π70π71π- 73π81π82π

Molecule	Atom 2 (C)	Atom 5 (C)	Atom 8 (C)	Atom 10 (O)
23 (67)	64π66π67π-69π72σ73σ	64π66π67π-68π69π70π	63π64π67π-68π70π71π	65π66π67π-69π76π77π
24 (67)	64π66π67π-69π73σ74σ	64π66π67π-68π69π70π	63π64σ67π-68π70π71π	65π66π67π-69π76π79π
25 (75)	72π74π75π-77π79σ82σ	72π74π75π-76π77π78π	72π73π75π-76π78π80π	73π74π75π-77π86π98π
26 (75)	72π74π75π-77π80σ82σ	72π74π75π-76π77π78π	71π72σ75π-76π78π79π	73π74π75π-77π85π96π
27 (63)	60π62π63π-65π66π69σ	60π62π63π-64π65π66π	59π60π63π-64π65π66π	61π62π63π-65π73π74π
28 (67)	64π66π67π-69π73σ74σ	64π66π67π-68π69π70π	63π64σ67π-68π70π71π	65π66π67π-69π76π77π
29 (71)	68π70π71π-73π77σ78σ	68π70π71π-72π73π74π	67π68π71π-72π74π75π	69π70π71π-73π81π98π
30 (71)	68π70π71π-73π77σ78σ	68π70π71π-72π73π74π	67π68π71π-72π74π75π	69π70π71π-73π81π83π
31 (79)	76π78π79π-81π83σ87σ	76π78π79π-80π81π82π	76π77π79π-80π82π84π	77π78π79π-81π90π112π
32 (79)	76π78π79π-81π84σ86σ	76π78π79π-80π81π82π	75π76π79π-80π82π83π	77π78π79π-81π90π100π
33 (39)	34π36π38π-41π44π46σ	37π38π39π-40π41π42π	36π37π39π-40π42π43π	37π38π39π-41π45π47π
34 (43)	40π42π43π-45π48σ49σ	40π42π43π-44σ45π46π	39π40π43π-44π46π47π	41π42π43π-45π51π52π
35 (47)	45π46π47π-49π51σ53σ	45π46π47π-48π49π50π	44π45π47π-48π50π51π	45π46π47π-49π55π 63π
36 (51)	48π50π51π-53π56σ57σ	48π50π51π-52π53π54π	46π47π51π-52π54π55π	49π50π51π-53π59π60π
37 (55)	52π54π55π-57π60σ61σ	52π54π55π-56π57π58π	51π52π55π-56π58π59π	53π54π55π-57π62π63π
38 (51)	45π48π50π-53π56σ57σ	48π50π51π-52π53π54π	47π48π51π-52π54π55π	49π50π51π-53π59π64π
39 (51)	48π50π51π-53π56π57σ	48π50π51π-52π53π54π	47π48σ51π-52π53π54π	49π50π51π-53π59π69π
40 (55)	52π54π55π-57π60σ61π	52π54π55π-56π57π58π	50π51π55π-56σ58π59σ	53π54π55π-57π63π66π
41 (55)	52π54π55σ57π60σ61σ	52π54π55π-56π57π58π	51π52π55π-56π58π59π	53π54π55π-57π64π72π
42 (59)	57π58π59π-61π64π65σ	57π58π59π-60π61π62π	56π57π59π-60π62π63π	57π58π59π-61π67π68π
43 (63)	59π62π63π-65π68σ70π	61π62π63π-64π65π66π	60π61π63π-64π66π67π	61π62π63π-65π72π 87π
44 (55)	52π54σ55π-57π58π60σ	52π54π55π-56π57π58π	51π52π55π-56π57π58π	53π54π55π-57π65π75π
45 (59)	51π56π58π-61π64π65σ	56π 58π 59-60π61π62π	54π55π59- 60π 62π 63π	57π58π59π-61π 69π75π
46 (63)	54π60π62σ-65π68σ70σ	60π62π63π-64π65π66π	58π59π63π-64π66π 67π	61π62π63π-65π73π74π
47 (59)	56π58σ59π-61π64σ65σ	56π58π59π-60π61π62π	55π56σ59π-60π62π63π	57π58π59π-61π67π76π
48 (63)	60π62π 63π-65π68σ70σ	60π62π63π-64π65π66π	59π60π63π-64π66π67π	61π62π63π-65π78π86π
49 (63)	60π62σ63π-65π69σ70σ	60π62π63π-64π65π66π	58π59π63π-64π66π67π	61π62π63π-65π72π84π
50 (67)	64π66π67π-69π73σ74σ	64π66π67π-68π69π70π	62π63π67π-68π70π71π	65π66π67π-69π77π88π

The results indicate that for these molecules the variation of the inhibition activity on neoplastic transformation is related to the variation of the numerical values of seven local atomic reactivity indices belonging to the common skeleton. The beta values (Table 2) show that the importance of the variables is $\varphi_{R2} >> \varphi_{R1} > F_{10}(LUMO)^* > F_5(LUMO+2)^* > F_8(HOMO-2)^* > Q_4^{max} > F_2(LUMO+1)^*$.

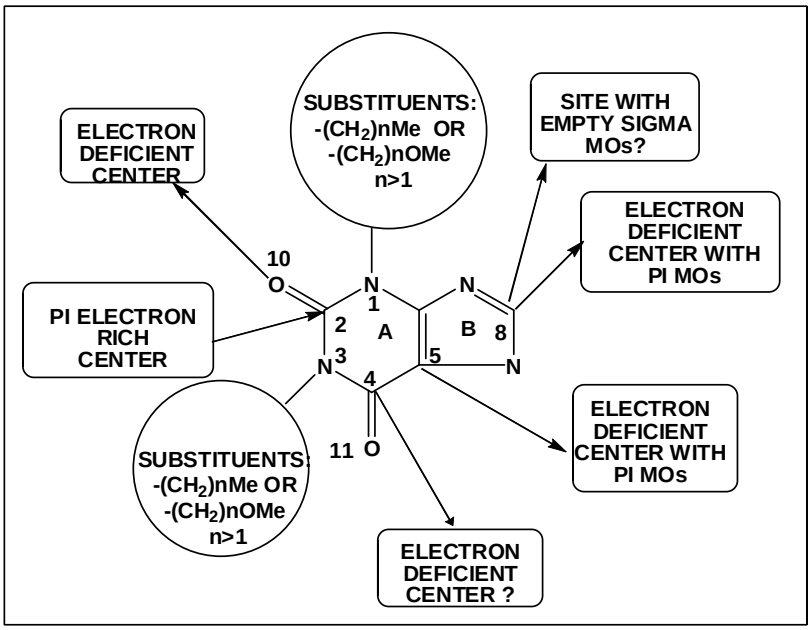

Fig. 4. Proposed partial 2D pharmacophore for the inhibitory activity of caffeine derivatives on neoplastic transformation

The process seems to be orientational parameters and orbital-controlled. We used variable-by-variable analysis (this is an approximation because the inhibition activity on neoplastic transformation depends simultaneously on all variables of the equation). We notice that the concerning variables are positives numerical values. So the good inhibition activity on neoplastic transformation is associated with high numerical values for φ_{R2}, φ_{R1}, $F_8(HOMO-2)*$, $F_2(LUMO+1)*$ and low numerical values for $F_{10}(LUMO)*$, $F_5(LUMO+2)*$ and Q_4^{max}.

A high value of means that the R2 substituent should have a high value of orientational parameter, but with similar electronic effects on the cycle. We suggest to use substituents such as $(CH_2)_nMe$, $(CH_2)_nOMe$ with n ≥ 1. The same is suggested for the R1 substituent. The maximal optimal size of both substituents cannot be calculated theoretically and it is necessary to wait for new experimental results. It is important to note that the beta value of φ_{R2} is higher than the other beta values. Therefore, selecting the most active molecule of Table 1 and trying several different R_2 substituents is a reasonable approach.

Atom 8 is carbon atom on ring B (Fig. 2). A high activity is associated with a high value of implying that $(HOMO-1)_8*$ and $(HOMO)_8*$ also participate. $(HOMO-1)_8*$ and $(HOMO-1)_8*$ have a π nature in almost all cases (Table 4). Therefore, we suggest that atom 8 should interact with a site that has empty π MOs. The participation of σ MOs can be explained by suggesting the possibility of a second interaction of the σ-π kind, but this is not clear. It is possible also that an ideal molecule has the three highest occupied local MOs with a π nature.

Atom 2 is a carbon atom on ring A (Fig. 2). A high value of $F_2(LUMO+1)*$ is associated with high activity. This suggests that $(LUMO+1)_2*$ interacts with an electron-rich center. $(LUMO)_2*$ also participates in the process. Table 4 shows that $(LUMO)_2^*$ has a π nature in all molecules. $(LUMO+1)_2*$ has a σ nature in most molecules. This strongly suggests that atom 2 could interact with a site having π occupied molecular orbitals and with an additional site having σ occupied MOs.

Atom 10 is an oxygen atom bond to the ring A (Fig. 2). A high activity is associated with a low value for $F_{10}(LUMO)*$. Table 4 shows that this MO has a π nature. Note that this MO does not coincide with the molecule's LUMO. A low value

for this index can be obtained by lowering the corresponding Fukui index. Another way is finding a substituent making that $(LUMO)_{10}$* coincides with some of the molecule's empty MOs other than (LUMO), (LUMO+1), (LUMO+2), etc. This suggests that atom 10 is interacting with an electron-deficient center through π-π stacked, π-π T-shaped and/or π-cation interactions.

Atom 5 is a carbon atom of rings A and B (Fig. 2). A low value of $F_5(LUMO+2)$* is associated with high activity. Table 4 shows that the three lowest empty MOs have a π nature in all molecules. The local $(LUMO)_5$* coincides with the molecule's LUMO. A possible suggestion is that atom 5 acts as an electron donor through π-π stacked, π-π T-shaped and/or π-cation interactions, and that $(LUMO+1)_5$* is engaged in a repulsive interaction with empty MOs of the site.

Atom 4 is carbon atom of ring A (Fig. 2). A low value of Q_4^{max} suggest that this atom is not prone to receive extra charge. Therefore atom 4 is probably facing an electron-deficient center.

This analysis allows us to propose the following partial 2D pharmacophore for the inhibition activity of caffeine derivatives on neoplastic transformation.

4. CONCLUSION

We have obtained statistically significant results relating the variation of the numerical values of a definite set of local atomic reactivity indices with the variation of the inhibitory activity on neoplastic transformation of caffeine derivative. Our model shows that the orientational parameters of two substituents on the ring A are important to explain this biological activity, so the length of the alkyl chain influences the activity of caffeine derivatives. This result agrees with the report of Rogozin [16]. The results should be useful to propose new molecules which have higher inhibitory effects on neoplastic transformation.

COMPETING INTERESTS

Authors have declared that no competing interests exist.

REFERENCES

1. Cancer fact sheet N°297. World Health Organization; 2017.
2. Bray F. Transitions in human development and the global cancer burden in World Cancer Report 2014. Editors Bernard W Stewart, Christopher P Wild. Lyon: Naturaprint; 2014.
3. Zhang L, Cai QY, Cai ZX, Fang Y, Zheng CS, Wang LL, Lin S, Chen DX, Peng J. Interactions of bovine serum albumin with anti-cancer compounds using a Proteon XPR36 array biosensor and molecular docking. Molecules. 2016;21:1706-15.
4. Eurtivong C, Semenov V, Semenova M, Konyushkin L, Atamanenko O, Reynisson J, Kiselyov A. 3-Amino-thieno[2,3-b]pyridines as microtubule-destabilising agents: Molecular modelling and biological evaluation in the sea urchin embryo and human cancer cells. Bioorganic & Medicinal Chemistry. 2017;25:658-64.
5. Clark R, Lee SH. Anticancer properties of capsaicin against human cancer. Anticancer Research. 2016;36:837-43.
6. Chiou CT, Lee WC, Liao JH, Cheng JJ, Lin LC, Chen CY, Song JS, Wu MH, Shia KS, Li WT. Synthesis and evaluation of 3-ylideneoxindole acetamides as potent anticancer agents. European Journal of Medicinal Chemistry. 2015;98:1-12.
7. Mahapatra DK, Bharti SK, Asati V. Anti-cancer chalcones: Structural and molecular target perspectives. European Journal of Medicinal Chemistry. 2015;98: 69-114. DOI:http://dx.doi.org/10.1016/j.ejmech.2015.05.004
8. Devi KP, Rajavel T, Habtemariam S, Nabavi SF, Nabavi SM. Molecular mechanisms underlying anticancer effects of myricetin. Life Sciences. 2015;142:19-25.
9. Nosaki K, Hamada K, Takashima Y, Sagara M, Matsumura Y, Miyamoto S, Hijikata Y, Okazaki T, Nakanishi Y, Tani K. A novel, polymer-coated oncolytic measles virus overcomes immune suppression and induces robust antitumor activity. Molecular Therapy Oncolytics. 2016;3:16022
10. Karpavičienė I, Valiulienė G, Raškevičius V, Lebedytė I, Brukštus A, Kairys V, Rūta N, Čikotienė I. Synthesis and antiproliferative activity of α-branched α,β-unsaturated ketones in human hematological and solid cancer cell lines. European Journal of Medicinal Chemistry. 2015;98:30-48.

11. Heffernan TP, Kawasumi M, Blasina A, Anderes K, Conney AH, Nghiem P. ATR-Chk1 pathway inhibition promotes apoptosis after UV in primary human keratinocytes: Potential basis for caffeine's UV protective effects. The Journal of Investigative Dermatology. 2009;129:1805-1815.
12. Lu G, Liao J, Yang G, Reuhl KR, Hao X, Yang CS. Inhibition of adenoma progression to adenocarcinoma in a 4-(Methylnitrosamino)-1-(3-Pyridyl)-1-Butanone–induced lung tumorigenesis model in A/J mice by tea polyphenols and caffeine. Cancer Research. 2006;66: 11494-11501.
13. Jiang W, Wu Y, Jiang X. Coffee and caffeine intake and breast cancer risk: An updated dose&#x response meta-analysis of 37 published studies. Gynecologic Oncology. 2013;129:620-629.
14. Arab L. Epidemiologic evidence on coffee and cancer. Nutr Cancer. 2010; 62: 271
15. Chen JC, Hwang JH. Effects of caffeine on cell viability and activity of histone deacetylase 1 and histone acetyltransferase in glioma cells. Tzu Chi Medical Journal. 2016;28:103-108.
16. Rogozin EA, Lee KW, Kang NJ, Yu H, Nomura M, Miyamoto KI, Conney AH, Bode AM, Dong Z. Inhibitory effects of caffeine analogues on neoplastic transformation: Structure-activity relationship. Carcinogenesis. 2008;29:1228.
17. Gómez Jeria JS. La Pharmacologie Quantique, Boll. Chim. Farmac. 1982;121: 619-25. French
18. Gómez-Jeria JS. On some problems in quantum pharmacology I. The partition functions. Int. J. Quant. Chem. 1983;23: 1969-72.
19. Gómez-Jeria JS. Modeling the drug-receptor interaction in quantum pharmacology in molecules. In Physics, Chemistry, and Biology, J. Maruani Editor, Netherlands: Springer; 1989.
20. Barahona-Urbina C, Nuñez-Gonzalez S, Gómez-Jeria JS. Model-based quantum chemical study of the uptake of some polychlorinated pollutant compounds by Zucchini subspecies. J. Chil. Chem. Soc. 2012;57:1497-503.
21. Bruna-Larenas T, Gómez-Jeria JS. A DFT and semiempirical model-based study of opioid receptor affinity and selectivity in a group of molecules with a morphine structural core. Int. J. Med. Chem. 2012;1-16. Article ID 682495
22. Gómez-Jeria JS. Elements of molecular electronic pharmacology. Ediciones Sokar, Santiago de Chile; 2013. Spanish
23. Gómez-Jeria JS. New set of local reactivity indices within the Hartree-Fock-Roothaan and density functional theory frameworks. Canad. Chem. Trans. 2013;1:25-55.
24. Gómez-Jeria JS, Flores-Catalán M. Quantum-chemical modeling of the relationships between molecular structure and *In vitro* multi-step, multimechanistic drug effects. HIV-1 Replication Inhibition and Inhibition of Cell Proliferation as Examples. Canadian Chemical Transactions. 2013;1:215-37.
25. Gómez-Jeria JS. Tables of proposed values for the orientational parameter of the substituent I. Monoatomic, Diatomic, Triatomic, n-CnH2n+1, O-n-CnH2n+1, NRR', and Cycloalkanes (With a Single Ring) Substituents. Res. J. Pharmac. Biol. Chem. Sci. 2016;7(2):288-94.
26. Gómez-Jeria JS, Robles-Navarro A. A DFT analysis of the inhibition of carbonic anhydrase isoforms I, II, IX and XII by a series of benzenesulfonamides and tetrafluorobenzenesulfonamides. American Journal of Chemistry and Applications. 2015;2:66.
27. Leal MS, Robles-Navarro A, Gómez-Jeria JS. A density functional study of the inhibition of microsomal prostaglandin E2 Synthase-1 by 2-aryl substituted quinazolin-4(3H)-one, pyrido[4,3-d]pyrimidin-4(3H)-one and pyrido[2,3-d]pyrimidin-4(3H)-one derivatives. Der Pharm. Lett. 2015;7:54-66.
28. Valdebenito-Gamboa J, Gómez-Jeria JS, A theoretical analysis of the relationships between electronic structure and HIV-1 integrase inhibition and antiviral activity of a series of naphthyridinone derivatives. Der Pharma Chem. 2015;7:543-55.
29. Bravo HR, Weiss-López BE, Valdebenito-Gamboa J, Gómez-Jeria JS. Res. J. Pharmac. Biol. Chem. Sci. 2016;7:792-98.
30. Gómez-Jeria JS, Abarca-Martínez S. A theoretical analysis of the cytotoxicity of a series of β-carbolinedithiocarbamate derivatives against prostatic cancer (DU-145), breast cancer (MCF-7), human lung adenocarcinoma (A549) and cervical

cancer (HeLa) cell lines. Der Pharma Chem. 2016;8:507-26.
31. Gómez-Jeria JS, Castro-Latorre P, Kpotin G. Quantum chemical analysis of the relationships between electronic structure and antiviral activity against HIV-1 of some Pyrazine-1,3-thiazine hybrid analogues. Der Pharma Chemica. 2016;8(20):234-39.
32. Gómez-Jeria JS, Cornejo-Martínez R. A DFT study of the inhibition of human phosphodiesterases PDE3A and PDE3B by a group of 2-(4-(1H-tetrazol-5-yl)-1H-pyrazol-1-yl)-4-(4-phenyl)thiazole derivatives. Der Pharma Chem. 2016;8: 329-37.
33. Gómez-Jeria JS, Gazzano V. A quantum chemical analysis of the inhibition of α-glucosidase by a group of oxadiazole benzohydrazone derivatives. Der Pharma Chem. 2016;8:21-7.
34. Gómez-Jeria JS, Matus-Perez M. A quantum chemical analysis of the inhibition of protein kinase A (PKA) and Rho-associated protein kinase-2 (ROCK2) by a series of urea-based molecules. Der Pharma Chem. 2016;8:1-11.
35. Gómez-Jeria JS, Moreno-Rojas C. A theoretical study of the inhibition of human 4-hydroxyphenylpyruvate dioxygenase by a series of pyrazalone-quinazolone hybrids. Der Pharma Chem. 2016;8:475-82.
36. Gómez-Jeria JS, Orellana Í. A theoretical analysis of the inhibition of the VEGFR-2 vascular endothelial growth factor and the anti-proliferative activity against the HepG2 hepatocellular carcinoma cell line by a series of 1-(4-((2-oxoindolin-3-ylidene)amino)phenyl)-3-arylureas. Der Pharma Chem. 2016;8:476-87.
37. Kpotin GA, Atohoun GS, Kuevi UA, Houngue-Kpota A, Mensah JB, Gómez-Jeria JS. A quantum-chemical study of the relationships between electronic structure and anti-HIV-1 activity of a series of HEPT derivatives. J. Chem. Pharmaceut. Res. 2016;8:1019-26.
38. Robles-Navarro A, Gómez-Jeria JS. A quantum-chemical analysis of the relationships between electronic structure and citotoxixity, GyrB inhibition, DNA supercoiling inhibition and anti-tubercular activity of a series of quinoline–aminopiperidine hybrid analogues. Der Pharma Chem. 2016;8:417-40.
39. Kpotin G, Atohoun SYG, Kuevi UA, Kpota-Hounguè A, Mensah JB, Gómez-Jeria JS. A quantum-chemical study of the relationships between electronic structure and trypanocidal activity against *Trypanosoma brucei brucei* of a series of thiosemicarbazone derivatives. Der Pharmacia Lettre. 2016;8(17):215-22.
40. Frisch MJ, Trucks GW, Schlegel HB, Scuseria GE, Robb MA, Cheeseman JR, Montgomery J, Vreven JAT, Kudin KN, Burant JC, Millam JM, Iyengar SS, Tomasi J, Barone V, Mennucci B, Cossi M, Scalmani G, Rega N. G03 Rev. E.01. Gaussian, Pittsburgh, PA, USA; 2007.
41. Gómez-Jeria JS. An empirical way to correct some drawbacks of mulliken population analysis. J. Chil. Chem. Soc. 2009;54:482-85.
42. Gómez-Jeria JS. D-Cent-QSAR: A program to generate local atomic reactivity indices from Gaussian 03 log files. v. 1.0. Santiago, Chile; 2014.
43. Statsoft. Statistica v. 8.0. 2300 East 14 th St. Tulsa, OK 74104, USA, 1984-2007.

Peer-review history:
The peer review history for this paper can be accessed here:
http://sciencedomain.org/review-history/18682